

Validation of Wave Spectral Partitions from SWIM instrument on-board CFOSAT against In-situ Data

Haoyu Jiang^{1,2*}, Alexey Mironov³, Lin Ren², Alexander V. Babanin⁴, Lin Mu^{1,5}

¹ Hubei Key Laboratory of Marine Geological Resources, China University of Geosciences, Wuhan, China

² State Key Laboratory of Satellite Ocean Environment Dynamics, Second Institute of Oceanography, Ministry of Natural Resources, Hangzhou, China

³ eOdyn, Plouzane, France

⁴ Melbourne School of Engineering, University of Melbourne, Melbourne, Australia

⁵ College of Life Sciences and Oceanography, Shenzhen University, Shenzhen, China

Corresponding author: Haoyu Jiang (Haoyujiang@cug.edu.cn)

Key Points:

- Partitioned integrated wave parameters (PIWPs) from the SWIM instrument onboard CFOSAT are validated against NDBC data.
- Comparison of two buoys close to each other shows that PIWP error metrics are functions of cross-assignment spectral distance threshold.
- CFOSAT SWIM performs well in estimating peak wave periods and directions but underestimates the energy of well-identified partitions.

Abstract

The Surface Waves Investigation and Monitoring (SWIM) instrument onboard the China France Oceanography Satellite (CFOSAT) can retrieve directional wave spectra with a wavelength range of 70~500 m. This study aims to validate the partitioned integrated wave parameters (PIWPs) from SWIM, including partitioned significant wave height (PSWH), peak wave period (PPWP), and peak wave direction (PPWD), against those from National Data Buoy Center (NDBC) buoys. With quasi-simultaneous spectra from two NDBC buoys 13 km away from each other near Hawaii, the methods of comparing PIWPs from two sets of spectra were discussed first. After cross-assigning partitions according to the spectral distance, it is found that wrong cross-assignments lead to many outliers strongly impacting the estimate of error metrics. Three methods, namely comparing only the best-matched partition, changing the threshold of spectral distance during cross-assignment, and maximum likelihood estimation of root-mean-square error (RMSE) of PIWPs, were used to reduce the impact of potential wrong cross-assignments. Using these methods, the SWIM PIWPs were validated against NDBC buoys. The results show that SWIM performs well at finding the spectral peaks of different partitions with the RMSE of PPWPs and PPWDs of 0.9 s and 20°, respectively, which can be a useful complement for other wave observations. However, the accuracy of PSWH from SWIM is not that good at this stage, probably because the high noise level in the spectra impacts the result of the partitioning algorithm. Further improvement is needed to obtain better PSWH information.

Plain Language Summary

The Surface Waves Investigation and Monitoring (SWIM) instrument onboard the China France Oceanography Satellite (CFOSAT) is the world's first space-borne 'wave spectrometer' which can provide directional spectra of wind-waves. After the launch of a sensor, it is necessary to validate its data product. However, the innovative wave spectrometer conception requires the development of new validation approaches. Particularly, we address to the problem of directional wave spectrum validation. First, we compared the data from two geographically close buoys to determine robust metrics for wave spectra inter-comparison. The use of the integrated wave parameters (IWP, e.g., wave height, wave period, and wave direction) of different wave systems seems to be a reasonable choice to characterize different sea states. After that, the spectra retrieved from SWIM were compared with those measured by buoys using our methods. The results show that the current spectra from SWIM can rightly capture the wave period and wave direction of different wave systems with small errors, which can be useful in the studies of oceanography and ocean engineering. However, the wave height information of each wave system still has a relatively large error. Improving this can be the future working direction of refinements of the SWIM wave spectrum retrieving algorithm.

1 Introduction

Wind-generated surface gravity waves (simply called waves henceforth) are a fundamental and ubiquitous phenomenon in the ocean. Waves are crucial for many aspects of human life (e.g., coastal engineering, seafaring, and port operations) and many geophysical

processes (e.g., momentum exchange, coastal erosion, and ice break in polar regions). Theoretical analyses, numerical models, and water tank experiments are all very useful tools to investigate waves and have helped the community to have a better understanding of this phenomenon. However, oceanography is a subject built based on observations. Wave observations in the ocean, no matter in situ or remote sensing observations, always play an irreplaceable role in related studies.

To better understand the waves in the ocean, the Surface Waves Investigation and Monitoring (SWIM) instrument, the first space-borne ‘wave spectrometer’ in the world, was successfully launched on China-France Oceanography SATellite (CFOSAT) on 29 October 2018. The SWIM instrument is a rotating 6-beam radar at small incidence angles operating at 13.575 GHz (Hauser et al., 2021). The main objective of SWIM is to provide directional wave spectra in the open ocean. The SWM instrument is able to not only obtain simultaneous nadir Significant Wave Height (SWH) and sea surface wind speed information like a radar altimeter, but also retrieve directional wave spectral information like a Synthetic Aperture Radar (SAR) working in the “wave mode” using its beams with small incidence angles (6~10°). Compared to SARs, SWIM does not have the so-called “azimuth-cutoff” problem and can resolve wavelengths from 70 m to 500 m (Hauser et al., 2021). Furthermore, SWIM can work synergistically with the wind scatterometer also onboard CFOSAT (Liu et al., 2020). These features make SWIM a very promising tool for the studies of ocean waves.

After a space-borne earth observation sensor is launched, a necessary procedure is to validate the data product. The correct understanding of uncertainties would determine the natural limits and possible scenarios of data application. In addition, some of the systematic errors of the retrievals can be corrected during this procedure. The general method for data validation is to collocate the remote sensing wave data with the reference data using a “spatial-temporal window” within which the wave parameters are assumed to be constant. Then comparisons can be carried out based on these match-ups. The reference data are usually data from in-situ instruments or other well-calibrated remote sensing systems (e.g., Ribal & Young, 2019).

The validation of remotely sensed Integral Wave Parameters (IWPs), such as SWH, Mean Wave Direction (MWD), and Mean Wave Period (MWP), is relatively simple and the method is relatively mature. Both wave buoys and well-calibrated altimeters can provide fairly reliable measurements of SWH, and are widely used in the validation of remotely sensed SWH (e.g., Liu et al., 2016; Jiang, 2020). When sufficient match-ups between two data sources are accumulated, the error metrics, such as bias, Root Mean Square Error (RMSE), and Correlation Coefficient (CC), can be used to evaluate the accuracy of the data:

$$Bias = \frac{1}{n} \sum_{i=1}^n (y_i - x_i) \quad (1)$$

$$RMSE = \sqrt{\frac{1}{n} \sum_{i=1}^n (y_i - x_i)^2} \quad (2)$$

$$CC = \frac{\sum_{i=1}^n (y_i - \bar{y})(x_i - \bar{x})}{\sqrt{\sum_{i=1}^n (y_i - \bar{y})^2} \sqrt{\sum_{i=1}^n (x_i - \bar{x})^2}} \quad (3)$$

where x and y represent the data from two sources; bars over them denote their mean values.

Validation of remotely sensed directional wave spectra from a space-borne sensor, such as those from SWIM, is more complicated. There seems to be no common approach for comparing two sets of directional wave spectra. Sometimes, the “effective” wave parameters, which are computed from the common range of wavelengths/frequencies of satellite and reference datasets, are used for the comparison. For instance, Mouche et al. (2016) and Wang et al. (2020) used effective SWH to evaluate the wave spectra from Sentinel-1A wave mode; Li and Holt (2009) and Li and Saulter (2012) used the SWH integrated from some certain frequency bands to evaluate the wave spectra from Envisat Advanced SAR (ASAR). The comparisons of overall SWH, MWP, and MWD are also based on this idea. However, while the agreement between the effective IWPs from two directional wave spectra is good, the two spectra can differ significantly, especially when more than one wave components coexist at the given location.

Although there are methods that evaluate directional wave spectra based on differences, correlations, and similarities between spectra (e.g., Hasselmann et al., 1996; Collins et al., 2014; Dabbi et al., 2015), the community still prefers the comparison of IWPs because their physical meanings are clearer (Ardhuin et al., 2019). As an intermediate solution, the wave spectra are often divided into different wave partitions using spectral partitioning algorithms (e.g., Hanson & Phillips, 2001; Portilla et al., 2009), and wave parameters are computed for each spectral partition. After that, the Partitioned IWPs (PIWPs) from different datasets can be compared. The comparison of spectral partitions has been used in the verification of wave spectral information from SAR (e.g., Mouche et al., 2016; Wang et al., 2020) and numerical wave model (NWM, e.g., Jiang et al., 2016; Delpy et al. 2010). If the PWIPs of wave partitions from satellite have a good agreement with those from the reference spectra, the remotely sensed wave partitions are considered good-quality and can be used in many studies focusing on a single wave system, such as data assimilation of NWMs (e.g., Hasselmann et al., 1996; Voorrips et al., 1997; Aouf et al., 2006, 2021) and tracking the evolution of wave systems (e.g., Ardhuin et al., 2009; Collard et al., 2009; Jiang et al., 2017a). However, for some studies concerning the relationship between two or more wave partitions, such as crossing seas/swells (Li, 2016), such a “partition-level” comparison is insufficient, because some energetic partitions might be missing and some partitions might be spurious in the remotely sensed spectra due to various reasons (Jiang et al., 2017b). Such cases of missing and wrongly identified partitions are often omitted in “partition-level” comparison.

Comparison has been made between the PIWPs from SWIM and those from numerical wave models (e.g., Hauser et al. 2021). However, because some physical processes are still not well parameterized in the NWMs (e.g., discrete interaction approximation for wave-wave interaction), the wave spectra from NWMs can be sometimes bad-quality even if it has a good performance on overall SWH (Cavaleri et al., 2007). The error of PWIPs in NWMs can also be large for high sea-states and low-frequency swell components (Liu et al., 2019; Jiang et al., 2016). Therefore, the comparison against in-situ measurements is also a common practice for the calibration and validation of ocean remote sensing data. The aim of this study is to validate the PIWPs from SWIM against data from the National Data Buoy Center (NDBC). Since there is no consensus on how PIWPs from two data sources should be compared, we used in-situ spectra from two buoys that are close in space distance to discuss this open question before the validation. The remainder of this manuscript is organized as follows: the data are described in Section 2. The method of comparing partitions from two sets of directional spectra was

discussed in Section 3. Section 4 gives the results for the comparison of PIWPs between SWIM and NDBC buoys, followed by the concluding remarks in Section 5.

2 Data

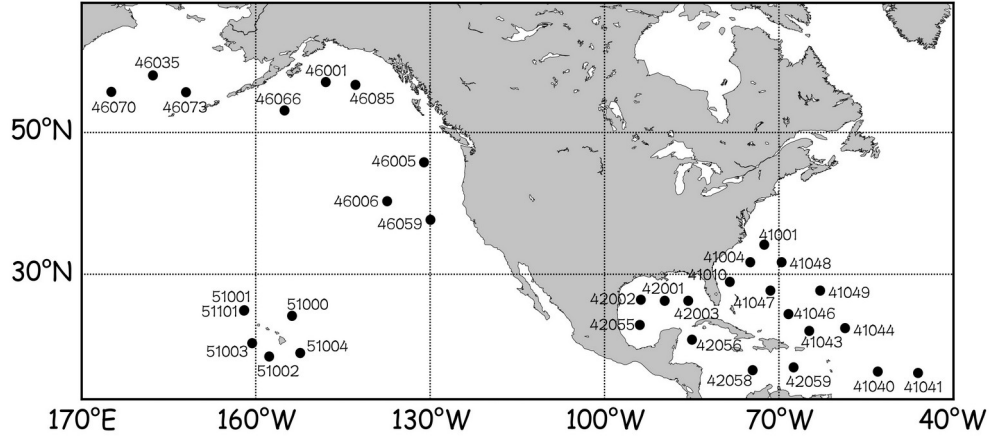
2.1 SWIM Wave Spectral Parameters

The directional wave spectra from the 6°, 8°, and 10° off-nadir beam as well as the “wave box” from Level-2 products of SWIM (version 5.1.2) from May 2019 to April 2020 (1 year) were evaluated in this study. These wave spectra were estimated from the Level-1b data using the method described in Hauser et al. (2021). Compared to previous versions of data, this version applied a new empirical speckle correction algorithm and no mask on the wave spectra, which improved the data quality. The obtained spectrum was segmented into up to three partitions using the method of Hanson and Phillips (2001), and the partitioned significant wave height (PSWH), partitioned peak wave period (PPWP), and partitioned peak wave direction (PPWD) were then computed for each partition. Here, we mainly focused on the above three PWIPs from SWIM because they are the most widely used parameters in the assimilation of observed wave spectra (e.g., Hasselmann et al., 1996; Voorrips et al., 1997; Aouf et al., 2021) and analyzing the evolution of ocean swells (e.g., Ardhuin et al., 2009; Collard et al., 2009; Jiang et al., 2017a). According to Hauser et al. (2021), validation of the PWIPs also minimizes the impact of the background noise of the SWIM instrument. The PPWL was converted to Partitioned Peak Wave Period (PPWP) using the dispersion relation, to compare with the results of wave frequency spectra from NDBC buoys. The water depth data used in the converting process was ETOPO2 (Earth TOPOgraphy 2 arc minutes). The records with signals from land, ice, or rain (these quality flags are available from the data) were not used in the comparison.

2.2 NDBC Buoy Data

The data from wave buoys that are far from the coasts are usually hired as the reference in the validation of wave remote sensing data (e.g., Liu et al., 2016; Jiang, 2020). Some buoys can provide the first five Fourier coefficients of waves from the translational or pitch-roll information. The first five Fourier coefficients are the minimum requirement for the reconstruction of the directional wave spectrum. The in-situ wave measurements from the NDBC coastal-marine automated network are widely used in the validation of wave remote sensing data and numerical wave models (e.g., Liu et al., 2016; 2019), thus, they were also used in this study. The NDBC data is quality-controlled and archived at the National Oceanographic Data Center (NODC). The data from May 2019 to April 2020 were selected using three criteria of buoys: (1) measuring the first five Fourier coefficients; (2) located more than 150 km offshore; (3) being with a water depth of more than 200 m. Over the selected period, 34 buoys meet these criteria, of which the locations are shown in Figure 1. The directional wave spectra were reconstructed using the maximum entropy method (Lygre and Krogstad, 1984). The reconstructed directional wave spectra can differ using different methods of reconstruction (Donelan et al., 2015), and sometimes the first five Fourier coefficients cannot resolve two partitions with similar periods and less than 60° apart of wave direction (Ardhuin et al., 2019). However, they are probably the best available spectra from a single buoy. Previous studies have also shown that the spectral partition information from NDBC buoys can be used to validate and correct outputs of NWMs (e.g., Jiang et al. 2016; Delpey et

193 al. 2010). The wave spectra were also partitioned using the method of Hanson and Phillips
 194 (2001) after smoothing using the method of Portilla et al. (2009). The PSWH, PPWP, and
 195 PPWD of up to four partitions were computed without identifying wind-seas and swells.



196
 197 **Figure 1.** The locations of the National Data Buoy Center (NDBC) buoys used in the study.

198 3 Comparing partitions from two spectra

199 3.1 Cross-assignment

200 There seems to be no consensus on how partitions from two sets of spectra should be
 201 compared. However, “cross-assignment” is an idea that has been used in the validation of
 202 spectral partition information from SAR (e.g., Mouche et al., 2016; Wang et al., 2020) and the
 203 assimilation of spectral partitions into NWM (e.g., Hasselmann et al., 1996; Aouf et al., 2006,
 204 2021). Given a partition in one wave spectrum, the aim of “cross-assignment” is to identify its
 205 corresponding partition in the other wave spectrum. In Hauser et al. (2021), two different cross-
 206 assignment methods were applied. One is to associate the wave partitions using their energy
 207 rank, that is, compare the 1st/2nd/3rd largest partitions in one spectrum with the 1st/2nd/3rd largest
 208 partitions in the other spectrum accordingly (hereafter, called the energy ranking method).
 209 However, the energy rank of partitions from two spectra will be different when there are
 210 missing or spurious peaks in one spectrum or when energy of two partitions is close in one
 211 spectrum. This will potentially lead to a large number of erroneous match-ups between
 212 partitions. It was shown by Jiang et al. (2017b) that only less than 1% of the records in
 213 Globwave ASAR dataset have the same 1st and 2nd swell partitions with their collocated
 214 WAVEWATCH III output. The second method in Hauser et al. (2021) is to cross-assign the
 215 two partitions with the smallest spectral distance (hereafter, simply called the nearest distance
 216 method), which provides more reasonable results. This technique can be used for not only
 217 comparing the partitions from two wave spectra (e.g., Wang et al., 2020) but also tracking
 218 wave systems generated by the same meteorological event (e.g., Jiang, 2019). In this study, the
 219 cross-assignment was conducted using the spectral distance defined as:

$$D = \sqrt{\left(\frac{T_a - T_b}{1_x} \right)^2 + \left(\frac{\theta_a - \theta_b}{\theta_{coef}} \right)^2} \quad (4)$$

220
 221 where T and θ are PPWP and PPWD, respectively, and the subscripts a and b denote the
 222 parameter from two different sources. θ_{coef} is a weighting factor that needs to be tuned and the

error metrics between two spectra are dependent on this parameter. There are other ways of defining spectral distance (e.g., Aouf et al., 2006; Delpey et al., 2010; Husson, 2012), and the selection of the definition depends, to a large extent, only on personal taste.

In the nearest distance method, the spectral distance is computed for each pair of partitions for two collocated wave spectra, and, and the pair of partitions (from different spectra) with the shortest spectral distance were cross-assigned. Then, two rest partitions with the shortest spectral distance are also cross-assigned, until all partitions from one spectrum are cross-assigned. The cross-assigned pair of partitions, if their spectral distance is short, can be regarded as the same wave system from two different data sources. The PSWHs, PPWPs, and PPWDs from the cross-assigned pair of partitions can then be used in the comparison and assessment.

To better demonstrate how cross-assignment works and to show some potential problems of these methods, we compared the wave partitions from two NDBC buoys in the open ocean of Hawaii region, 51001 and 51101, located only ~13 km away from each other during May 2019 to April 2020. The representativeness error between them should be very small so that the data from the two buoys also provide an opportunity to investigate the noises and errors of wave data from NDBC buoys, which is regarded as the reference in this study. Figure 2a and 2b are the wave spectra obtained at UTC1700 May 9, 2019, from buoy 51001 and 51101, respectively. The original buoy wave spectra are noisy and the agreement between the two spectra seems not to be good with a Correlation Coefficient (CC) between the spectral grid points of 0.56. Figure 2c shows the CC of spectral density at each spectral bin during the selected period between the spectra from the two buoys. The CCs in Figure 2c are less than 0.6 in most spectral bins, also indicating bad agreement between the spectra of the two buoys. However, after the 3×3 spectral bin smoothing using Portilla et al. (2009), the agreement between the two spectra (Figure 3d and 3e) becomes much better (CC = 0.91). The CCs of spectral density also increase to more than 0.8 for most spectral bins (Figure 3f). A similar condition occurs when calculating the RMSEs of spectral grid points (not shown). This indicates that the methods based on CCs or RMSEs (e.g., Hasselmann et al. 1996) of spectral grid points are probably not a good method to quantitatively evaluate the agreement between two wave spectra, especially when the data are noisy.

Despite the good agreement in Figures 2d and 2e, not all partitions from the two spectra can be rightly cross-assigned. The PSWHs, PPWPs, and PPWDs derived from the two spectra are shown as circles and triangles in Figure 2f. For both spectra, four partitions are identified. Table 1 shows the information of identified partitions in the two spectra. Partitions are identified in both spectra at $\sim\langle 340^\circ, 0.09\text{Hz} \rangle$, and the spectral distance between them is the shortest so that they were first cross-assigned (regarded as the same partition). Partitions are also identified in both spectra at $\sim\langle 45^\circ, 0.17\text{Hz} \rangle$, and they were subsequently cross-assigned. The third shortest spectral distance is between the partition at $\sim\langle 180^\circ, 0.08\text{Hz} \rangle$ from buoy 51001 and the partition at $\sim\langle 150^\circ, 0.08\text{Hz} \rangle$ from buoy 51101. The two partitions were cross-assigned despite the $\sim 30^\circ$ difference of wave directions. The partitions at $\sim\langle 90^\circ, 0.11\text{Hz} \rangle$ and $\sim\langle 350^\circ, 0.16\text{Hz} \rangle$ are only identified in buoy 51001 and 51101, respectively. However, according to the rule of cross-assignment, these two partitions also need to be cross-assigned even if they cannot be regarded as the same partition at all. If the energy ranking method is used, the two partitions ($\sim\langle 90^\circ, 0.11\text{Hz} \rangle$ for 51001 and $\sim\langle 350^\circ, 0.16\text{Hz} \rangle$ for 51101) will still be wrongly cross-assigned.

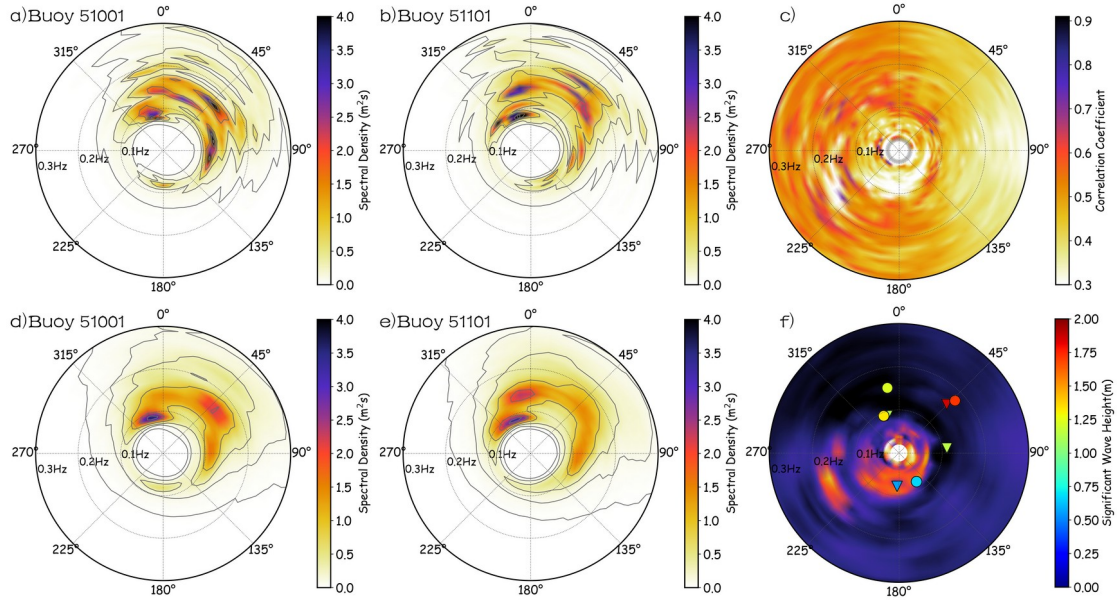


Figure 2. Directional wave spectra obtained at UTC1700 May 9, 2019 from the buoy (a) 51001 and (b) 51101, and (c) the CC of spectral density between spectra from the two buoys over the period from May 2019 to April 2020. (d, e, f) is the same as (a, b, c), but after smoothing in spectral space. Subplot (c) and (f) use the same color bar in (c). The triangles and circles in (f) represent the partitions derived from the spectra from buoy 51001 and 51101, respectively. The colors of triangles and circles indicate PSWHs and the locations of them indicate PPWPs and PPWDs.

Such conditions of wrong cross-assignment occur frequently because missing or spurious partitions are common in both observed and modelled wave spectra. The comparison of the cross-assigned PSWH, PPWP, and PPWD between the two buoys over the selected period are shown in Figure 3a-c. In Figure 3, θ_{coef} was set to 25° during the comparison of buoy partitions (The reason for selecting this value is described later in this section). The biases are negligible for all three partitioned parameters. For PSWH, the RMSE is 0.30 m and the CC is 0.94, which seems to be an acceptable accuracy. For PPWP, although the agreement is also generally good between the two buoys, there are many outliers in Figure 3b due to the aforementioned wrong cross-assignment, increasing the RMSE and reducing the CC. A similar condition is also observed in Figure 3c where the outliers from wrong cross-assignment lead to a large “random” error. Meanwhile, the discrepancies of PWIPs between two buoys seem to be small if these outliers due to wrong cross-assignment are not considered. One method to get rid of most of these outliers is to only cross-assign the partitions with the minimum spectral distance for each pair of spectra, which was used in Wang et al. (2020). The agreement between the two buoys can be very good if we only consider one partition from one spectrum: For PSWH (Figure 3d), PPWP (Figure 3e), and PPWD (Figure 3f), the RMSEs (CCs) can reach 0.24 m (0.97), 0.33 s (0.99), and 8.7° (1.00), indicating that the good-quality partitions from buoy spectra can be a good reference for validating other data. However, this method underestimates the errors of PWIPs because the partitions with larger errors of PPWD and PPWP are not considered in this case. The results can only be regarded as the upper limit of the precision of buoy partitions.

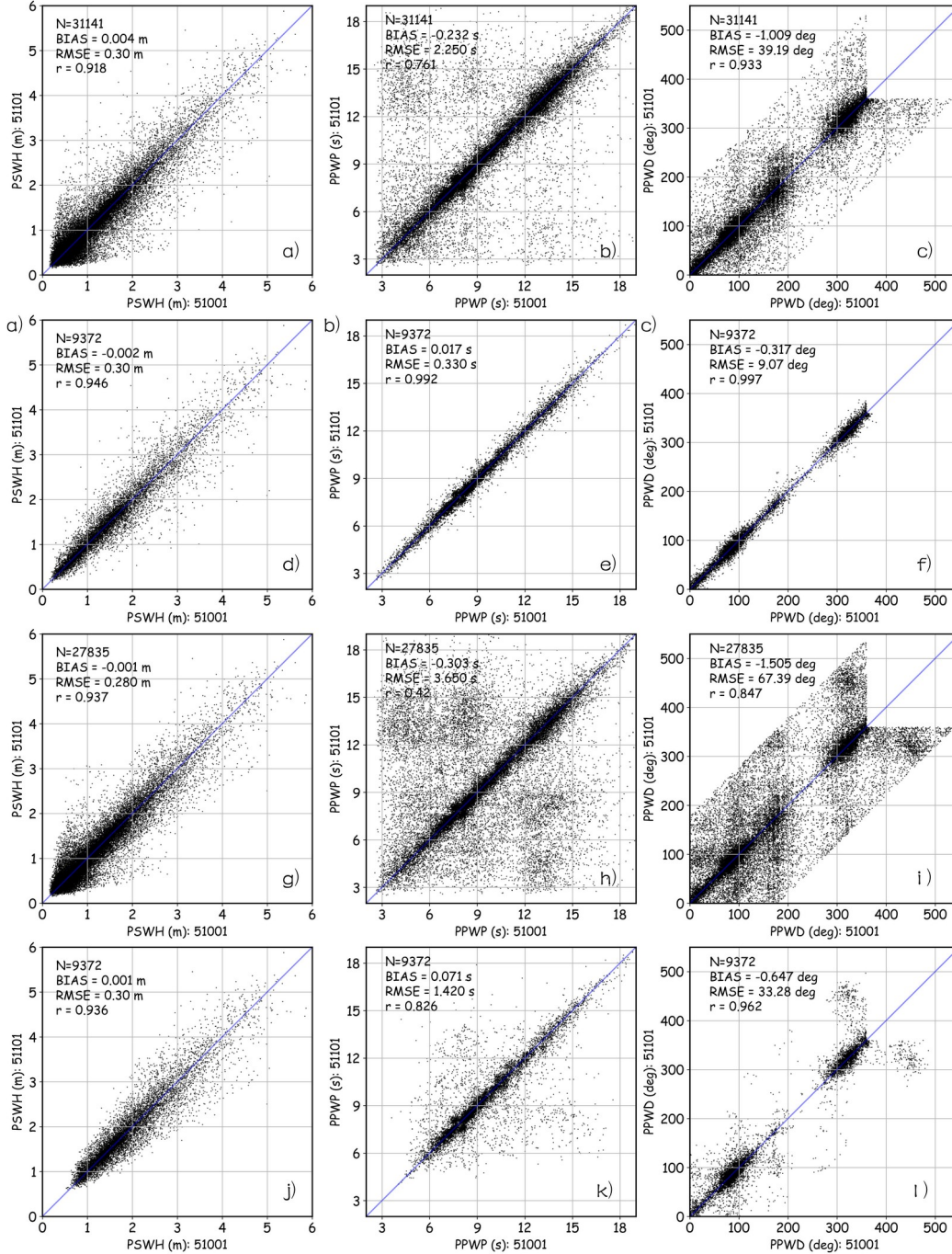
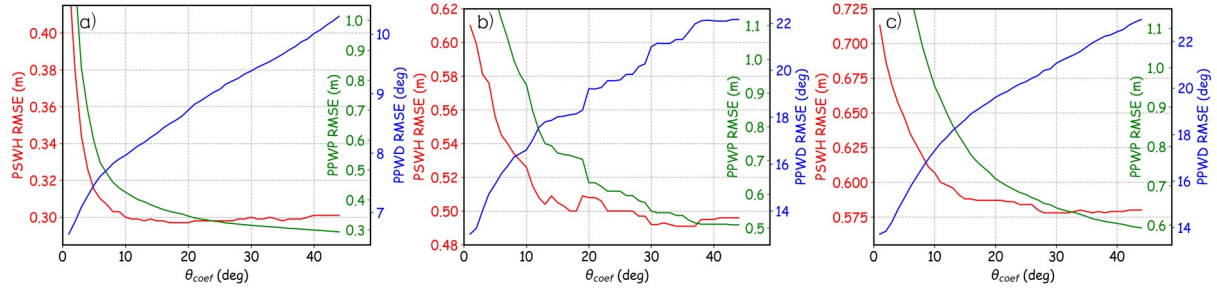


Figure 3. Comparison of PWIPs (left column: PSWH, middle column: PPWP, right column: PPWD) between buoy 51001 and 51101 over the period from May 2019 to April 2020. (a-c) All partitions are cross-assigned using the nearest distance method; (d-f) Only partitions with the minimum spectral distance for each pair of spectra are cross-assigned using the nearest distance method; (g-i) All partitions are cross-assigned using the energy ranking method; (j-l) Only the most energetic partition (the 1st partition) at each spectrum is compared.

Because comparing only the best-matched partitions can reduce the impact of outliers, the value of factor θ_{coef} in Equation 4 was also selected based on this method. Figure 4a shows

RMSEs of PIWPs between the two buoys for only best-matched partitions as a function of θ_{coef} . The RMSE of PPWD increases with the increase of θ_{coef} while the RMSE of PPWP decreases with the increase of θ_{coef} . When θ_{coef} is small, the RMSE of PSWH also decreases with the increase of θ_{coef} . Meanwhile, the gradients of PSWH and PPWP along with θ_{coef} decrease with the increase of θ_{coef} . When θ_{coef} changes from 10° to 40° , the RMSE of PSWH stays almost unchanged (~ 0.3 m), and the RMSEs of PPWP and PPWD also vary only in a relatively small range ($0.3\sim 0.4$ s for PPWP RMSE and $8^\circ\sim 10^\circ$ for PPWD RMSE). Therefore, the above $\theta_{coef} = 25^\circ$ is able to give relatively stable estimates of RMSEs of PIWPs.



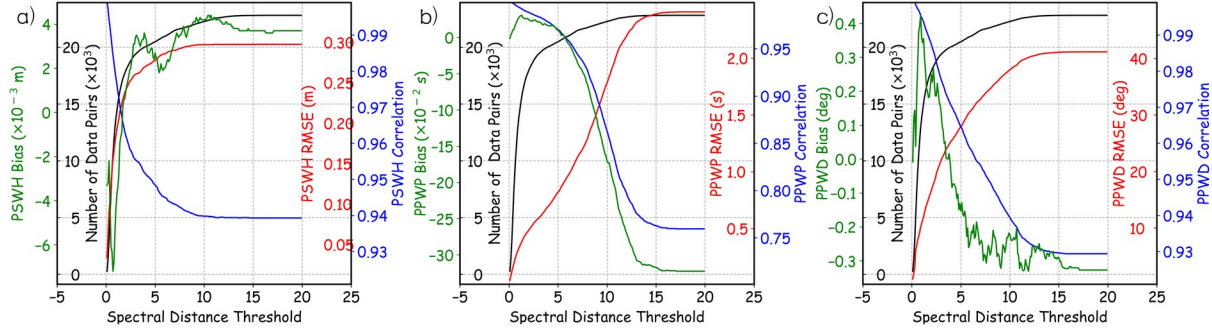
314

Figure 4. RMSEs of PSWH (red), PPWP (green), and PPWD (blue) for best-matched partitions as a function of θ_{coef} in Equation 4: (a) between buoys 51101 and 51001, (b) between SWIM (10° beam) and NDBC buoys with a spatial window of 50 km, and (c) between SWIM (10° beam) and NDBC buoys with a spatial window of 200 km.

We also demonstrate the results of cross-assignment using the energy ranking method, and the full results are shown in Figure 3g-i. Although this method slightly reduced the RMSE (from 0.30 m to 0.28 m) of PSWH compared to the nearest distance method, the RMSEs and numbers of outliers of PPWP and PPWD both increased significantly. If we only compare the 1st partition, the results are better (Figure 3j-l), but the condition of wrong cross-assignment still occurs a lot. These outliers are because the 1st partition in one spectrum does not necessarily correspond to the 1st partition in the other spectrum when the energy of the 1st and 2nd partitions are close. Therefore, we avoided the use of energy ranking method in this study hereafter.

Using a threshold of D during cross-assignment seems to be a feasible method for removing the outliers during the comparison of partitions from two spectra. This approach is widely used in the assimilation of NWMs (e.g., Aouf et al., 2021). However, such a threshold needs to be treated with care during the evaluation of PIWPs, especially when the inaccuracies of PIWPs are unknown. This is because the number of outliers is so large that the computed error metrics are sensitive to the selection of the threshold. Figure 5 shows the numbers of cross-assigned data pairs, biases, RMSEs, and CCs of PIWPs as functions of the spectral distance threshold. Changing this threshold from 1 to 10, the RMSEs (CCs) of PSWH, PPWP, and PPWD change from 0.2 m (0.98), 0.4 s (0.99), and 10° (0.99) to 0.3 m (0.94), 1.7 s (0.87), and 37° (0.94), respectively. In such a condition, these error metrics lose their ability to represent the accuracy of data because they are strongly controlled by the selection of the threshold, especially for PPWP and PPWD. Such a problem also occurs when comparing partitions from two different data sources (e.g., buoy versus SWIM), and these outliers were also observed in Hauser et al. (2021) where PIWPs from SWIM were compared with PIWPs from an NWM. It seems to be difficult to eliminate the impact of these outliers due to the imperfection of buoy spectra (also SWIM spectra). However, curves in Figure 5 themselves

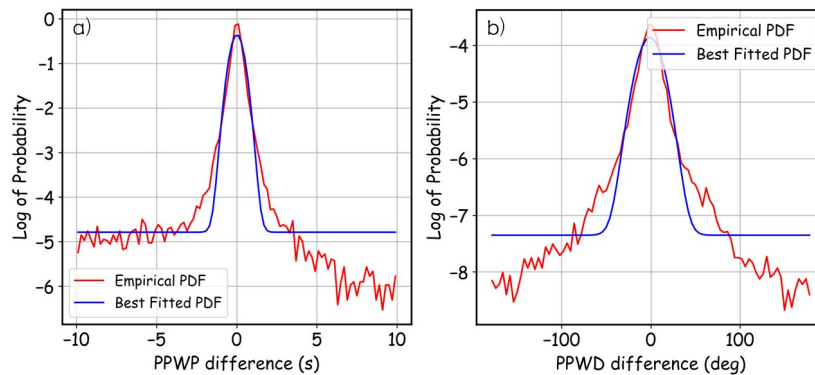
can illustrate how error metrics change with the selection of cross-assignment threshold D , which are helpful for applications such as data assimilation. Therefore, they can also serve as a tool to demonstrate the comparison between the partitions from two sets of wave spectra. We recommend using them in the comparison of PIWPs between cross-assigned partitions from different sources of wave spectra.



349

Figure 5. Number of cross-assigned data pairs (black), bias (green), RMSE (red), and CC (blue) of (a) PSWH, (b) PPWP, and (c) PPWD between buoy 51001 and 51101 as a function of spectral distance threshold for cross-assignment.

The distributions of PPWP and PPWD errors of outliers seem to be uniform from Figures 3b and 3c. Meanwhile, it is well known that the measurement error usually follows a normal distribution. Therefore, an assumption can be made that the errors in Figure 3b (3c) are the superposition of a normal distribution $U(a, b)$ and a uniform distribution $N(\mu, \sigma^2)$, where a and b define the range of the normal distribution that can be arbitrarily selected (but should include sufficient outliers), and μ and σ are the bias and RMSE of PPWPs (or PPWDs), respectively. Base on this assumption, the maximum likelihood method can be used to derive that the RMSEs of PPWP and PPWD are ~ 0.5 s and $\sim 10^\circ$, respectively, which is an acceptable accuracy to evaluate the SWIM data. The empirical and best-fitted probability density functions (PDFs) of PPWP and PPWD differences between the two buoys are shown in Figure 6. While the tails are not well fitted, the peaks have a good agreement between the empirical and best-fitted PDFs, indicating it is reasonable to estimated RMSEs of errors using this method.



366

Figure 6. PDFs of (a) PPWP and (b) PPWD difference between buoy 51001 and 51101 over the study period. The red lines are empirical PDFs and the blue lines are best-fitted PDFs assuming that the errors are normally distributed and the outliers are uniformly distributed. The y-axis is in log-scale.

3.2 Relationship between First Two Partitions

Some studies need to use the relationship between two partitions in one wave spectrum. For example, the energy ratio and direction difference between the 1st and 2nd partitions is crucial in the studies of crossing seas (e.g., Li, 2016). Jiang et al. (2017b) showed that the relationship between two partitions in one set of spectra can differ from that in the other set when some partitions are missing or spurious in one set of spectra. These problems cannot be identified using the cross-assignment method in Section 3.1. However, there is no universal method to compare between two spectra with respect to the relationship among different partitions. In this study, we used the PSWH ratio, PPWP difference, and PPWD difference between the 1st and 2nd partitions to evaluate whether the relationship between two partitions is well-represented by SWIM spectra. The reasons for selecting the 1st and 2nd partitions is that they have the highest signal-to-noise ratio and are of great interest in the studies of crossing seas.

The comparisons of PSWH ratio, PPWP difference, and PPWD difference between the 1st and 2nd partitions between buoy 51001 and 51101 are shown in Figure 7. Most points lie near the $y=x$ line, but many outliers are observed, which is not surprising because of the aforementioned reason that the 1st and 2nd partitions in one spectrum do not necessarily correspond to the 1st and 2nd partitions in the other spectrum, respectively. Meanwhile, the asymmetry of data is good along the $y=x$ line, also showing a good agreement between the two buoys.

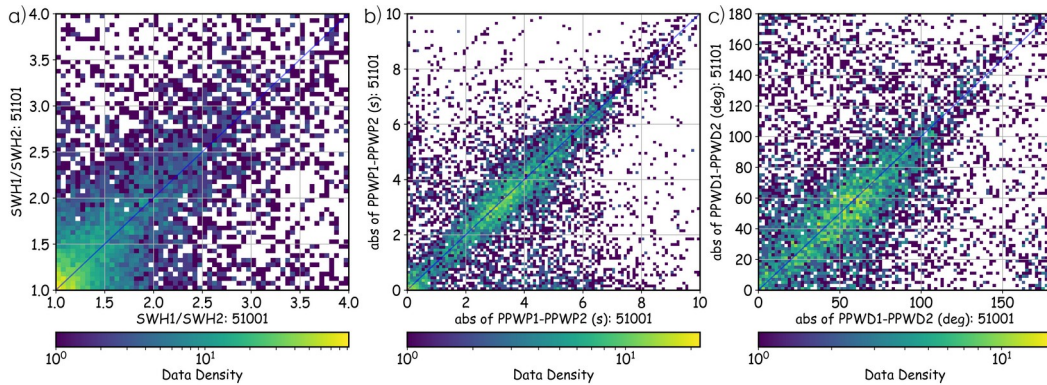


Figure 7. Comparison of (a) PSWH ratio, (b) PPWP difference, and (c) PPWD difference between the 1st and 2nd partitions between buoy 51001 and 51101 over the period from May 2019 to April 2020.

4 Validation of SWIM Partitions

4.1 Results of Cross-assignment

In this section, the SWIM PIWPs were validated against buoy data using the methodology in Section 3. Following previous studies of calibrating and validating SWH from altimeters (e.g., Ribal & Young, 2019; Liu et al. 2016), a spatial window of 50 km and a temporal window of 30 min were first selected when collocating buoy and SWIM spectra. The θ_{coef} in Equation 4 was still set to 25° because this value can provide generally stable estimates of RMSE for best-matched partitions (Figure 4b). This spatial-temporal window yields 360~391 collocations of wave spectra for different beams and “wave box”. Because SWIM cannot resolve the wavelength less than 70m, the buoy partitions with PPWP less than 5 s were

removed. The PPWDs of buoy partitions were converted to 0~180° because of the 180° ambiguity of SWIM spectra. For the best-matched partitions, the error metrics of PIWPs from different beams and the “wave box” were listed in Table 1. The agreements are generally good for PPWPs and PPWDs. The biases for the two parameters are small for all three beams and the wave box. The performances of 10° and 8° beams are similar with respect to identifying spectral peaks with an RMSE of ~0.6 s for PPWP and an RMSE of ~20° for PPWD, and the 10° beam performs slightly better than the 8° beam. In contrast, the 6° beam has the largest error with respect to all the three PIWPs. These are generally in line with the results of Hauser et al. (2021) in which the 10° beam also has the best performance among the three. The “wave box” does not perform better than the 8° beam although it is the combination of three beams. Compared to PPWPs and PPWDs, the bias of PSWHs are very significant (more than 0.3 m) for all three beams, indicating that the PSWHs from SWIM are underestimated compared to buoy.

Table 1. Error metrics of PIWPs from different beams and the “wave box” of SWIM for the best-matched partitions (only partitions with the minimum spectral distance for each pair of spectra are cross-assigned) compared to buoy data from May 2019 to April 2020.

	Beam 6°	Beam 8°	Beam 10°	Wave Box
No. Collocation	371	367	360	391
PSWH RMSE	0.66 m	0.60 m	0.61 m	0.63 m
PPWP RMSE	0.74 s	0.62 s	0.60 s	0.69 s
PPWD RMSE	23.2°	20.4°	20.4°	21.3°
PSWH Bias	0.46 m	0.35 m	0.36 m	0.33 m
PPWP Bias	-0.16 s	-0.16 s	-0.11 s	-0.19 s
PPWD Bias	-2.5°	-2.9°	-3.5°	-2.7°
PSWH CC	0.92	0.91	0.91	0.92
PPWP CC	0.96	0.97	0.97	0.96
PPWD CC	0.86	0.85	0.85	0.86

Because the 10° beam has the best performance among the three, the following analysis was mainly conducted using the data from the 10° beam to save space. The results for full cross-assignment of 10° beam are shown in Figure 8a-c, and the comparisons of only the best-matched partitions are shown in Figure 8d-f. The bias, RMSE, and CC of PSWH between SWIM and buoys are 0.16 m, 0.54 m, and 0.85, respectively. Surprisingly, the RMSE and bias of PSWH are lower in Figure 8a for full cross-assignment than in Figure 8d for best-matched cross-assignment. Similar to the condition in Figure 3b-c, many outliers exist in Figure 8b-c due to wrong cross-assignment, making the RMSE very large.

The small sample size of collocations in Figure 8 cannot yield a stable estimation of error metrics like in Figures 5 and 6, thus, a larger number of collocations are needed. To obtain more collocations between buoys and remote sensing measurements, Husson (2012) developed an innovative dynamic validation method by propagating the partitioned swell packet derived from satellites forward to the vicinity of buoys using the deep-water dispersion relation. Using this method, the remote sensing data relatively far from the buoy can be sometimes used for the comparison, which enlarges the number of collocation. However, this method has several problems: (1) The remotely sensed partitions with relatively large errors in PPWD cannot rightly propagate to the vicinity of buoys. Only the data with an accurate PPWD are validated so that the results are not sufficiently representative; (2) A “point source” model is used to estimate the evolution of wave height, which is found to be often inaccurate (Jiang et al.,

2017a); (3) If the propagation distance is large, a small error of the initial PPWP might lead to a large error of arrival time, which then leads to large errors of PWIPs. An alternative way of is back-propagating the partitioned swell packet from buoy to the vicinity of remote sensing observations. This method can avoid the aforementioned problem (1), but (2) still exists and (3) becomes a new problem: a small error of the initial PPWD from buoys might lead to large errors of arrival location. Therefore, despite its innovation, we do not recommend using this dynamic validation method.

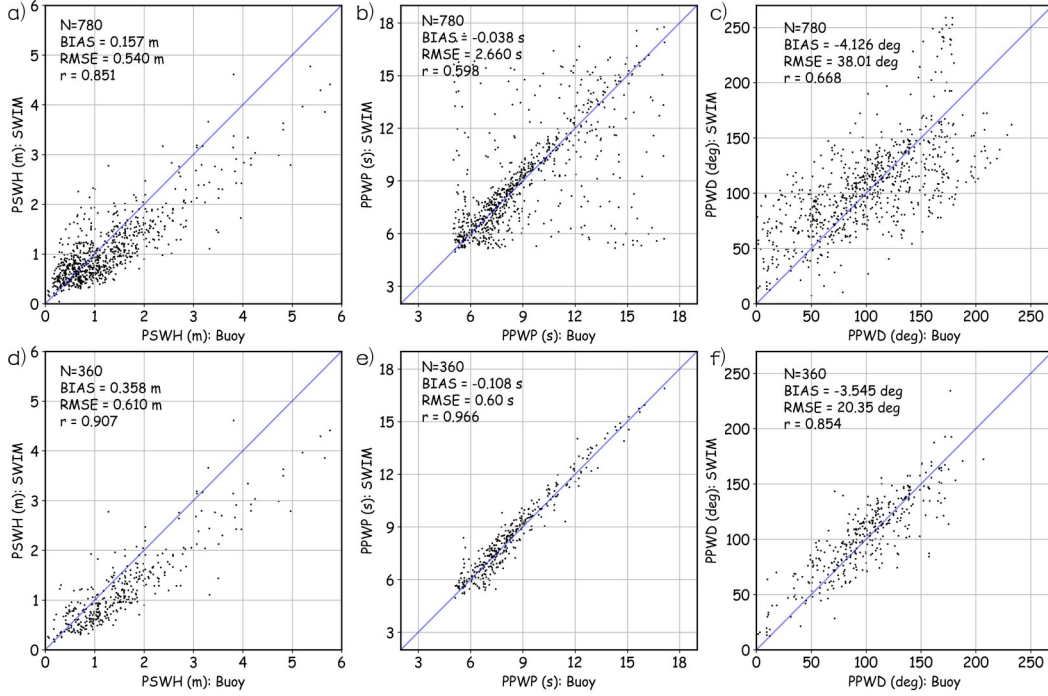
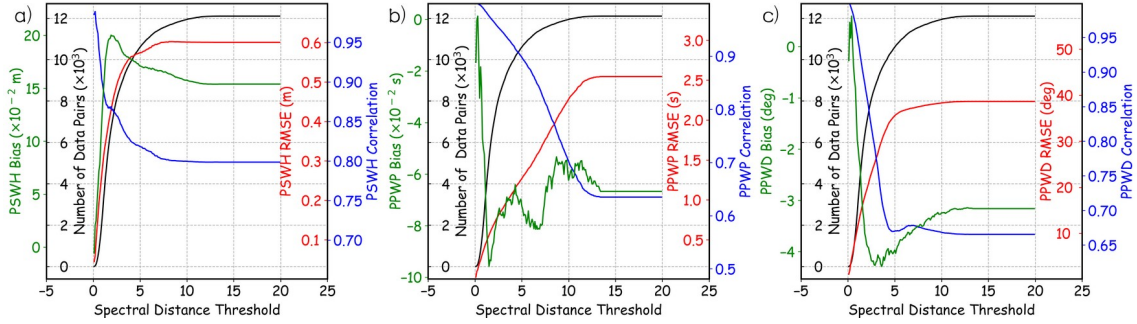


Figure 8. Comparison of PWIPs (left column: PSWH, middle column: PPWP, right column: PPWD) between SWIM 10° beam and buoys over the period from May 2019 to April 2020. (a-c) All partitions are cross-assigned; (d-f) Only partitions with the minimum spectral distance for each pair of spectra are cross-assigned.

Simply using a larger spatial window might be a better solution as the representativeness error can be estimated by changing the window size. We enlarged the spatial-temporal window for collocation to 200 km, which increased the number of collocated spectrum pairs to 5462. After enlarging the spatial-temporal window, the RMSE of the three PIWPs all slightly increased due to a larger representativeness error. In Figure 4c, the derived RMSEs become smoother but higher for each θ_{coef} , and the RMSEs of PSWH, PPWP, and PPWD are 0.6 m, 0.7 s, and 21°, respectively, when $\theta_{coef} = 25^\circ$. From the differences of RMSEs with different spatial collocation window, the representativeness error (in RMSE) can be roughly estimated that is ~0.1 m for PSWH, ~0.1 s for PPWP, and ~1° for PPWD. However, the bias of PSWH stays almost unchanged, confirming that the PSWHs from SWIM are systematically higher than those from buoys.

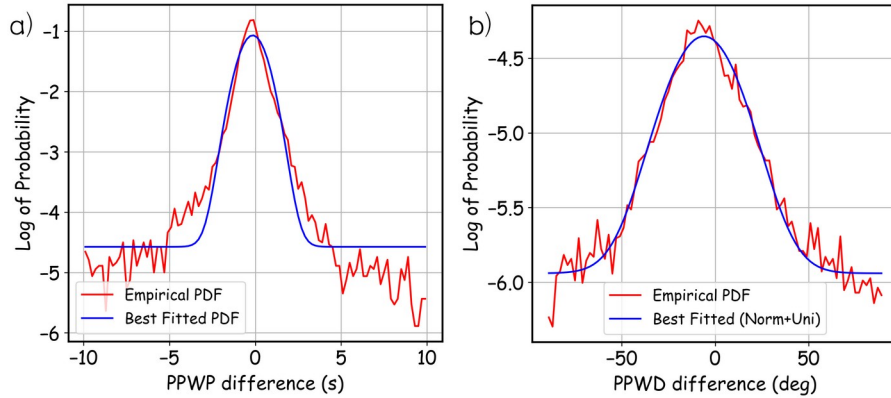
When the collocation spatial window is set to 200 km, the numbers of cross-assigned data pairs, biases, RMSEs, and CCs of PIWPs as functions of spectral distance threshold are shown in Figure 9. Similar to the condition in Figure 4, the RMSEs increase, and the CCs decrease significantly with the increase of the threshold for all three variables. Similarly, if one regards

the outliers in Figure 8 as a uniform distribution and the random errors as a normal distribution, it can be estimated using the maximum likelihood method that the RMSEs (biases) of PPWP and PPWD between SWIM and buoy partitions are ~ 0.95 s (~ -0.1 s) and $\sim 22^\circ$ (-6°), respectively. It can be observed from Figure 10 that the agreements are good between the empirical and best-fitted PDFs for both PPWP and PPWD differences. Considering the representativeness error, the actual RMSE of PPWPs and PPWDs between SWIM and buoys should be ~ 0.9 s and $\sim 21^\circ$, respectively.



473

Figure 9. Number of cross-assigned data pairs (black), bias (green), RMSE (red), and CC (blue) of (a) PSWH, (b) PPWP, and (c) PPWD between collocated spectra from SWIM 10° beam and NDBC buoy as a function of spectral distance threshold for cross-assignment. The size of the spatial window of collocation is 200 km for this figure.

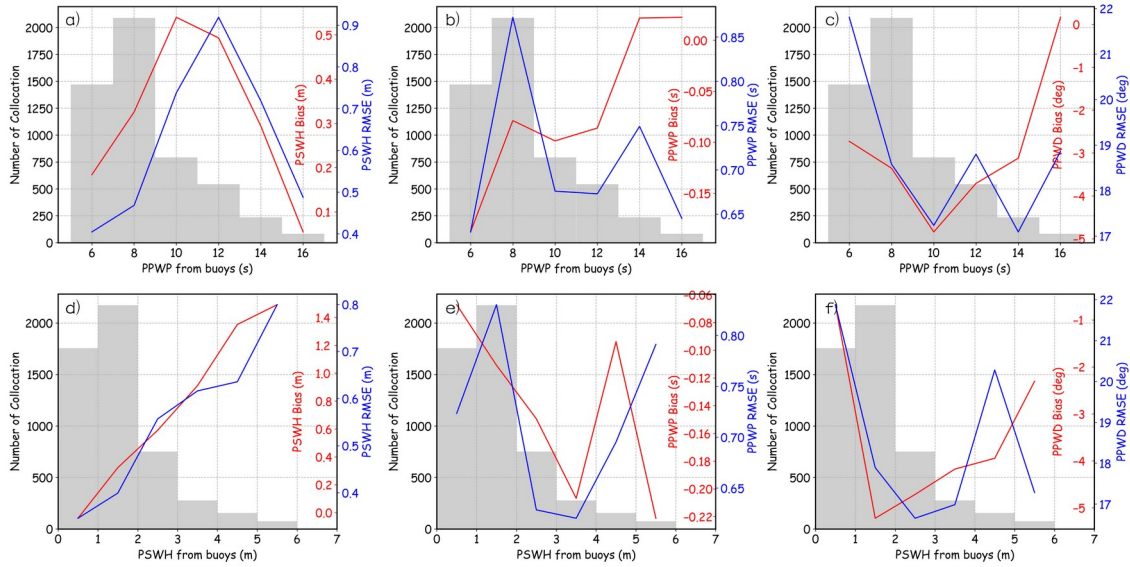


478

Figure 10. PDFs of (a) PPWP and (b) PPWD difference between partitions from SWIM 10° beam and from NDBC buoys over the study period. The red lines are empirical PDFs and the blue lines are best-fitted PDFs assuming that the errors are normally distributed and the outliers are uniformly distributed. The y-axis is in log-scale.

A larger number of collocations from a larger spatial-temporal window also provides an opportunity to examine the dependency of the bias and RMSE of PIWPs on buoy PSWHs and buoy PPWPs. The biases and RMSEs of PIWPs within each 1-m buoy PSWH bin and each 2-s buoy PPWP bin were computed, and the results are shown in Figure 11. Only the data from the 10° beam was used because it gives the best results (almost in all bins) among the three beams. Because the number of collocations is small in each PSWH or PPWP bin, we only computed the biases and RMSEs for the best-matched cases. The results in Figures 11a and 11d indicate that the SWIM underestimate the PSWH for all PPWPs and PSWHs. Such an underestimation is prominent when PPWP is 9~13 s (the corresponding bias of PSWH is ~ 0.5 m). The PSWH

RMSE of the SWIM is the highest when PPWP is ~ 12 s. Meanwhile, both the bias and RMSE of PSWH from the SWIM increase with the increase of the buoy PSWH (Figure 11d), which is similar to the condition of RMSE for SWHs from altimeters (e.g., Jiang, 2020). For errors of SWIM PPWP (Figures 11b and 11e), no clear pattern can be observed. This is probably because the numbers of collocations are too low (less than 250) to generate stable statistics when PPWP is higher than 13 s or when PSWH is higher than 4 m. For errors of SWIM PPWD (Figures 11c and 11f), the RMSE is the largest ($\sim 22^\circ$) when PPWP is less than 7 s or when PSWH is less than 1 m. For PPWPs larger than 7 s or PSWHs larger than 1 m, the average RMSE of PPWD is only $\sim 18^\circ$. Considering that the spatial-temporal representativeness error is small for PPWP ($\sim 1^\circ$), this result indicates that the overall PPWD RMSE of SWIM is less than 20° for waves with a PPWP of more than 8 s.



503

504 **Figure 11.** Biases (red) and RMSEs (blue) of PIWPs (left: PSWH, middle: PPWP, right: 505 PPWD) from SWIM (10° beam) for each (a-c) 2-s bin of buoy PPWPs and (d-f) 1-m bin of 506 buoy PSWH. The gray bars indicates the number of collocations in each 2-s or 1-m bin.

507 For PPWPs and PPWDs, a linear calibration between SWIM and buoy partitions can 508 eliminate the bias. A simple linear regression was used for the best-matched partitions and a 509 Theil-Sen regression was used for the “full” cross-assignments to avoid the impact of outliers. 510 The two methods give almost the same result, but the RMSEs of PPWP and PPWD are almost 511 not changed after the calibration (not shown). Considering the biases are small, there seems to 512 be no need to re-calibrate the PPWP and PPWD information from SWIM. Meanwhile, 513 considering the relatively large bias in PSWH, it can be deduced that a linear regression of 514 SWIM PSWH against buoy PSWH can significantly reduce the RSME. However, in this 515 version of SWIM data, the total energy of wave spectrum is corrected using the relatively 516 accurate nadir SWH so that the bias of overall SWH of a SWIM spectrum cannot be that large, 517 as shown in Figure 12a. Therefore, a simple linear calibration will lead to a significant 518 overestimate of overall SWH.

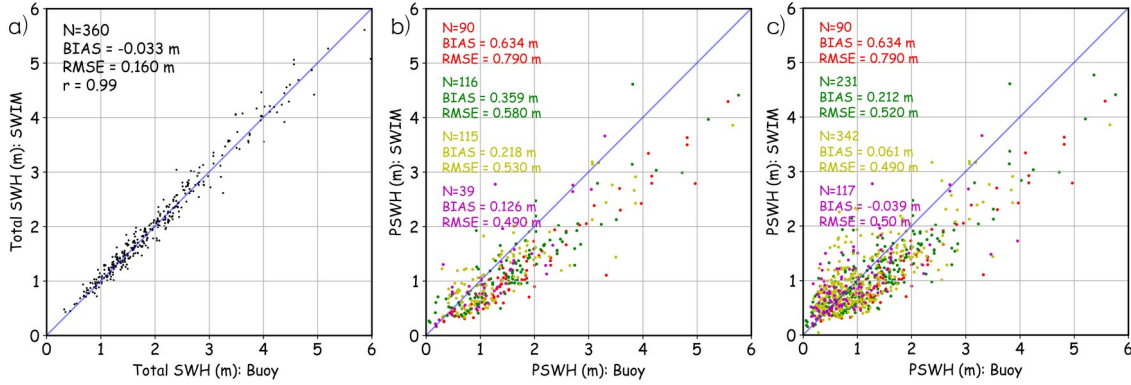


Figure 12. Comparison of SWH between SWIM 10° beam and buoys: (a) Total SWH, (b) PSWH for best-matched partitions, and (c) PSWH for all cross-assigned partitions. The colors of dots and texts in (b) and (c) indicate the number of partitions identified in the collocated buoy spectra (red: one partition, green: two partitions, yellow: three partitions, purple: four partitions).

It is likely that the bias comes from the spectral partitioning. In the 360 buoy spectra collocated with SWIM in Figure 8, there are 90, 116, 115, and 39 cases that one, two, three, and four partitions were identified by the partitioning algorithm, respectively. For the corresponding SWIM spectra, there are 357 cases that three partitions were identified. Therefore, fewer partitions were identified in the buoy spectra on average, although more partitions were allowed in the partitioning of buoy spectra. Given the certain overall energy, fewer partitions usually mean more energy in each partition, which is the reason for the underestimation of SWIM PSWH compared to buoys. For the best-matched partition (Figure 12b), the bias decreases with the increase of identified buoy partitions, confirming that less identified partitions in buoy spectra can lead to a larger bias. However, even for the condition that the number of partitions in buoy spectra are three and four, the PSWHs of best-matched partitions from SWIM are still underestimated for 0.22 m and 0.13 m, respectively. When two spectral partitions are separated using the watershed algorithm, the PSWH of the partition with higher energy tends to be underestimated when the spectral distance between the two partitions is short, because a part of its tail might be regarded as the energy belonging to the partition with lower energy. When the difference of PPWD between two well-separated partitions is larger than 90°, the 180° folding (ambiguity) of the SWIM spectrum will shorten the spectral distance between the two partitions, leading to the overlap of spectra and underestimation and overestimation of the partition with higher and lower energy, respectively. Most best-matched partitions in the condition that three and four partitions are identified have relatively larger energy than the rest. That is why the PSWHs of SWIM are often underestimated in the best-matched cases even if the buoys have equal or even more partitions. If all cross-assigned partitions are considered, the bias of SWIM PSWHs is negligible when the number of buoy partitions is three or four (Figure 12c). Therefore, when different numbers of partitions are identified in two spectra, the comparison of PSWHs needs to be treated with care. Although this error can be regarded as systematic, we failed to find any way to solve this problem at this stage, because the partitioning results depend not only on the partitioning algorithm but also on the noise level and accuracy of spectra. A potential solution can be a posteriori method, that is, to partition the spectrum with the partition contours of another spectrum to guarantee the same number of partitions. However, posteriori partitioning results can only be obtained from

NWMs in most conditions, and the spectra from NWMs can also be erroneous sometimes. Moreover, a 180° folding of the NWM spectrum is needed before partitioning, which might introduce more errors to the partitioning results.

4.2 Relationship of First Two Partitions

The comparison of PSWH ratio, PPWP difference, and PPWD difference between the 1st and 2nd partitions between SWIM and buoys are shown in Figure 13. The results are not as good as the comparison between the two buoys in Figure 7. For the PSWH ratio, there are only a few values from SWIM that are more than 2.5, but many values are more than 3 in the buoy data. This might be due to the aforementioned problem that SWIM tends to underestimate and overestimate the energy of more and less energetic partitions, respectively. For PPWP and PPWD differences, the correlations between SWIM and buoy results are also bad. This is because the 1st and 2nd partitions in one spectrum do not necessarily correspond to the 1st and 2nd partitions in the other spectrum, and this problem seems to be serious in the comparison between SWIM and buoy. This condition is similar to the problem in Globwave ASAR partitions which is identified in Jiang et al. (2017b). Therefore, we do not recommend using PIWPs in this version of SWIM data product to do wave climate studies, such as computing the occurrence probability of crossing seas.

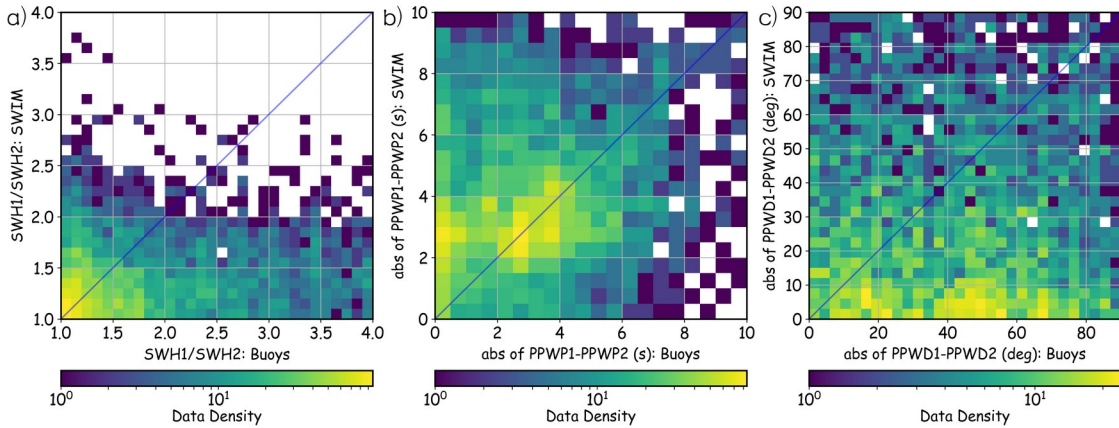


Figure 13. Comparison of (a) PSWH ratio, (b) PPWP difference, and (c) PPWD difference between the 1st and 2nd partitions between SWIM 10° beam and NDBC buoys over the period from May 2019 to April 2020. The size of the spatial window of collocation is 200 km for this figure.

5 Concluding Remarks

The SWIM instrument onboard the CFOSAT is a ‘wave spectrometer’ that can retrieve directional wave spectra with a wavelength range of 70~500 m. This study tried to evaluate the PIWPs, including PSWHs, PPWPs, and PPWDs, from the SWIM product of directional wave spectra against NDBC buoys. The methods of comparing PIWPs from two sets of spectra were discussed using two NDBC buoys that are close to each other. The comparison of the PIWPs between two buoys indicates that:

- 1) Cross-assignment of two partitions according to their spectral distance (the nearest spectral distance method) is better than cross-assignment according to their energy rank (the energy ranking method), because the nearest spectral distance method is less sensitive to the

conditions that there are missing or spurious partitions and the energy of two partitions are close to each other.

2) Even for the nearest spectral distance method, wrong cross-assignments occur frequently because missing or spurious partitions are common in both observed and modelled wave spectra. These wrong cross-assignments lead to many outliers making it difficult to evaluate the error metrics of PPWPs and PPWDs between two sets of spectra.

3) Wrong cross-assignments occur much less frequently if one only compares the best-matched partitions from each pair of spectra. For the best-matched partitions, the RMSEs of PPWPs and PPWDs are ~ 0.3 s and $\sim 9^\circ$, respectively, but they can only be regarded as the lower limit of RMSEs.

4) The threshold of spectral distance during cross-assignment, which seems to be a feasible method for removing the above outliers due to wrong cross-assignment, should be treated with care because the error metrics of PIWPs are functions of the value of the threshold. Meanwhile, plotting the curve of these functions can be helpful to evaluate the error.

5) It is feasible to estimate the RMSE of PPWPs and PPWDs using the maximum likelihood method assuming the residuals of reasonable data and outliers are normally and uniformly distributed, respectively. Using this method, it is estimated that the RMSE of PPWPs and PPWDs are ~ 0.5 s and $\sim 10^\circ$, respectively, which is a good precision.

6) The PSWH ratios, PPWP differences, and PPWD differences between the 1st and 2nd partitions are consistent in the data of the two buoys, indicating that these parameters from the buoy can also be used to validate spectra from other data sources.

Taking into account these points, the PIWPs from the SWIM instrument were validated against NDBC buoys. Because the widely used 50-km spatial window can only yield 360 collocations of spectra, a spatial window of 200 km was also used in some cases. The main results and conclusions of this part includes:

1) Using the best-matched comparison, it was estimated that the lower limits of RMSEs of PPWPs and PPWDs from SWIM are ~ 0.6 s and $\sim 20^\circ$, respectively. Using the aforementioned maximum likelihood method, it was estimated that the RMSEs of PPWPs and PPWDs from SWIM (10° beam, which performs the best among the three beams) are ~ 0.9 s and $\sim 20^\circ$, respectively. Both results indicate the SWIM has a good performance with respect to finding the spectral peaks of partitions.

2) The accuracy of PSWH from SWIM is not that good, although they are significantly correlated to the PSWH from buoys. The RMSE of PSWH between SWIM and buoys (~ 0.6 m) is much larger than the RMSE of overall SWH (< 0.2 m), and the SWIM tends to underestimate the energy of well-identified partitions (the bias is ~ 0.35 m). But this cannot be easily calibrated because the calibration of PSWH will impact the overall SWH of the spectrum.

3) On average, fewer partitions can be identified from buoys than from SWIM, which is the potential reason for this underestimation. Another potential reason is that the 180° ambiguity in SWIM spectra shortens the spectral distance among partitions, causing underestimation of partitions with relatively large energy.

4) In any case, using the PSWH data from SWIM in this version of data (version 5.1.2) need to be careful. For example, the PSWH ratios, PPWP differences, and PPWD differences

between the 1st and 2nd partitions from SWIM are also not consistent with those from buoys because of the relatively large errors in PSWH.

The results showed that SWIM is able to provide much useful information on wave spectra and their partitions. Particularly, with respect to finding the spectral peak of different wave systems, SWIM can have an accuracy of less than 1 s of PPWP and 20° of PPWD (PPWP > 7 s), which can be a useful complement for other wave observation methods and can be helpful for the assimilation of NWMs. The recent results of assimilation experiments also confirm this conclusion (Aouf et al. 2021). Meanwhile, the PSWHs from SWIM do not compare well with buoy at this stage, which is an important direction for improving the SWIM data quality. It is possible that the performance of PSWHs from SWIM can be improved in the future by improving the modulation transfer function to retrieve the spectra and partitioning algorithm, and by correcting the whole spectra against some reference data using advanced empirical methods, such as deep learning that is popular in the recent years.

Meanwhile, it is noteworthy that the reference dataset used in this study, the wave spectra from NDBC buoys, also has some limitations. First, as mentioned in Section 2, the reconstructed directional spectra from the first five Fourier coefficients have some problems. Second, due to their spatial sparseness, only 360 collocations of spectra were obtained using 1-year SWIM data with a spatial window of 50 km. Therefore, the validation of SWIM spectra can also benefit from better and more in-situ measurements of directional wave spectra. For example, a distributed wave sensor network that can provide the first five Fourier coefficients in many locations in the open ocean has been established using drifters (Smit et al. 2021), which might provide an opportunity to further validate and even improve the spectral information from SWIM.

Acknowledgments

HJ would like to thank Prof. Danièle Hauser and Dr. Jiuke Wang for the helpful discussion. This work is jointly supported by the Key-Area Research and Development Program of Guangdong Province (No. 2020B1111020005), the National Natural Science Foundation of China (41806010, U2006210), and Laboratory for Regional Oceanography and Numerical Modeling, Qingdao National Laboratory for Marine Science and Technology (2019A03).

Data Availability Statement

The SWIM data is available from the AVISO website: <https://www.aviso.altimetry.fr/en/data/products/wind/wave-products/wave-wind-cfosat-products.html>. The NDBC data are available from the NODC website: <https://www.ncei.noaa.gov/access/marine-environmental-buoy-database/DOC/general-buoy-netcdf.html>.

References

- Aouf, L., Lefevre, J.-M., & Hauser, D. (2006). Assimilation of Directional Wave Spectra in the Wave Model WAM: An Impact Study from Synthetic Observations in Preparation for the SWIMSAT Satellite Mission. *Journal of Atmospheric and Oceanic Technology*, 23, 448–463.

- Aouf, L., Hauser, D., Chapron, B., Toffoli, A., Tourain, C., & Peureux, C. (2021). New directional wave satellite observations: Towards improved wave forecasts and climate description in Southern Ocean. *Geophysical Research Letters*, 48, e2020GL091187. <https://doi.org/10.1029/2020GL091187>
- Ardhuin, F., Chapron, B., & Collard, F. (2009). Observation of swell dissipation across oceans. *Geophysical Research Letters*, 36, 1–5.
- Ardhuin, F., Stopa, J. E., Chapron, B., Collard, F., Husson, R., Jensen, R. E., et al. (2019). Observing Sea States. *Frontiers in Marine Science*, 6, 124.
- Cavaleri, L., Alves, J. H. G. M., Ardhuin, F., Babanin, A., Banner, M., Belibassakis, K., et al. (2007). Wave modelling - The state of the art. *Progress in Oceanography*, 75, 603–674.
- Collard, F., Ardhuin, F., & Chapron, B. (2009). Monitoring and analysis of ocean swell fields from space: New methods for routine observations. *Journal of Geophysical Research: Oceans*, 114, 1–15.
- Collins, C. O., Lund, B., Waseda, T., & Graber, H. C. (2014). On recording sea surface elevation with accelerometer buoys: lessons from ITOP (2010). *Ocean Dynamics*, 64, 895–904.
- Dabbi, E. P., Haigh, I. D., Lambkin, D., Hernon, J., Williams, J. J., & Nicholls, R. J. (2015). Beyond significant wave height: A new approach for validating spectral wave models. *Coastal Engineering*, 100, 11–25.
- Delpy, M. T., Ardhuin, F., Collard, F., & Chapron, B. (2010). Space-time structure of long ocean swell fields. *Journal of Geophysical Research: Oceans*, 115, 1–13.
- Donelan, M., Babanin, A., Sanina, E., & Chalikov, D. (2015). A comparison of methods for estimating directional spectra of surface waves. *Journal of Geophysical Research: Oceans*, 12, 5040–5053.
- Hanson, J., & Phillips, O. (2001). Automated analysis of ocean surface directional wave spectra. *Journal of Atmospheric and Oceanic Technology*, 18, 277–293.
- Hasselmann, S., Bruning, C., Hasselmann, K., & Heimbach, P. (1996). An improved algorithm for the retrieval of ocean wave spectra from SAR image spectra. *J. Geophys. Res.*, 101, 16615–16629.
- Hauser, D., Tourain, C., Hermozo, L., Alraddawi, D., Aouf, L., Chapron, B., et al. (2021). New Observations From the SWIM Radar On-Board CFOSAT: Instrument Validation and Ocean Wave Measurement Assessment. *IEEE Transactions on Geoscience and Remote Sensing*, 59, 5–26.
- Husson, R. (2012). Development and validation of a global observation-based swell model using wave mode operating Synthetic Aperture Radar. *PhD Thesis, Dep. of Earth Sci., Univ. of Bretagne Occidentale, Brest, France*.
- Jiang, H. (2019). Spatially tracking wave events in partitioned numerical wave model outputs. *Journal of Atmospheric and Oceanic Technology*, 36, 1933–1944.
- Jiang, H. (2020). Indirect validation of ocean remote sensing data via numerical model: An example of wave heights from altimeter. *Remote Sensing*, 12. <https://doi.org/10.3390/rs12162627>
- Jiang, H., Babanin, A. V., & Chen, G. (2016). Event-based validation of swell arrival time. *Journal of Physical Oceanography*, 46, 3563–3569.
- Jiang, H., Babanin, A. V., Liu, Q., Stopa, J. E., Chapron, B., & Chen, G. (2017a). Can contemporary satellites estimate swell dissipation rate? *Remote Sensing of Environment*, 201. <https://doi.org/10.1016/j.rse.2017.08.037>
- Jiang, H., Mouche, A., Wang, H., Babanin, A. V., Chapron, B., & Chen, G. (2017b). Limitation of SAR quasi-linear inversion data on swell climate: An example of global crossing swells. *Remote Sensing*, 9. <https://doi.org/10.3390/rs9020107>
- Li, J.-G., & Holt, M. (2009). Comparison of Envisat ASAR Ocean Wave Spectra with Buoy and Altimeter Data via a Wave Model. *Journal of Atmospheric and Oceanic Technology*, 26, 593–614.
- Li, J. G., & Saulter, A. (2012). Assessment of the updated Envisat ASAR ocean surface wave spectra with buoy and altimeter data. *Remote Sensing of Environment*, 126, 72–83.
- Li, X. M. (2016). A new insight from space into swell propagation and crossing in the global oceans. *Geophysical Research Letters*, 43, 5202–5209.
- Liu, J., Lin, W., Dong, X., Lang, S., Yun, R., Zhu, D., et al. (2020). First Results From the Rotating Fan Beam Scatterometer Onboard CFOSAT. *IEEE Transactions on Geoscience and Remote Sensing*, 58, 8793–8806.
- Liu, Q., Alexander, B., Changlong, G., Stefan, Z., Sun, J., & Jia, Y. (2016). Calibration and Validation of HY-2 Altimeter Wave Height. *Journal of Atmospheric and Oceanic Technology*, 33, 919–936.
- Liu, Q., Rogers, W. E., Babanin, A. V., Young, I. R., Romero, L., Zieger, S., et al. (2019). Observation-Based Source Terms in the Third-Generation Wave Model WAVEWATCH III: Updates and Verification. *Journal of Physical Oceanography*, 49, 489–517.
- Lygre, A., & Krogstad, H. E. (1984). Maximum Entropy Estimation of the Directional Distribution in Ocean Wave Spectra. *Journal of Physical Oceanography*, 16, 2052–2060.

- 726 Mouche, A., Wang, H., Husson, R., Guitton, G., Chapron, B., & Li, H. (2016). 2D ocean waves spectra from
 727 space: a challenge for validation and synergetic use. *Proc. SPIE 9878, Remote Sensing of the Oceans and*
 728 *Inland Waters: Techniques, Applications, and Challenges*, 98780L. <https://doi.org/10.1117/12.2227178>
- 729 Portilla, J., Ocampo-Torres, F. J., & Monbaliu, J. (2009). Spectral partitioning and identification of wind sea and
 730 swell. *Journal of Atmospheric and Oceanic Technology*, 26, 107–122.
- 731 Ribal, A., & Young, I. R. (2019). 33 years of globally calibrated wave height and wind speed data based on
 732 altimeter observations. *Scientific Data*, 6, 77. <https://doi.org/10.1038/s41597-019-0083-9>
- 733 Smit, P. B., Houghton, I. A., Jordanova, K., Portwood, T., Shapiro, E., Clark, D., et al. (2021). Assimilation of
 734 significant wave height from distributed ocean wave sensors. *Ocean Modelling*, 101738.
 735 <https://doi.org/https://doi.org/10.1016/j.ocemod.2020.101738>
- 736 Voorrips, A. C., Makin, V. K., & Hasselmann, S. (1997). Assimilation of wave spectra from pitch-and-roll buoys
 737 in a North Sea wave model. *Journal of Geophysical Research: Oceans*, 102, 5829–5849.
- 738 Wang, X., Husson, R., Jiang, H., Chen, G., & Gao, G. (2020). Evaluation on the capability of revealing ocean
 739 swells from sentinel-1a wave spectra measurements. *Journal of Atmospheric and Oceanic Technology*, 37,
 740 1289–1304.